Segmentation of Capillaroscopic Images

K. TUTUNCU[1] and M. BUBER[1]

[1] Selcuk University, Konya/Turkey, ktutuncu@selcuk.edu.tr
[1]Selcuk U
niversity, Konya/Turkey, mbuber@selcuk.edu.tr

***Abstract*- Capillaroscopy device shoot videos of capillaries of oral mucosa and nailfold of patient over the related skin without any pain. The image frames of videos are used by experts for early detection or treatment of some diseases such as diabetics, rheumatism and etc. Since this process is implemented in manually, decision support systems that helps the experts for diagnosis have been subjects of studies of biomedical researches. First step of these systems is the successful segmentation process on these images that will be used for classification of disease depending on 8 parameters such as the number of capillaries in a certain area, the distance between the two vessels, the size of the capillaries and etc. This study aims to contribute decision support system for experts by presenting a successful segmentation. In this study Otsu, Fuzzy C-mean, Fast Marching, Region Growing and H-Minima methods have been used for segmentation of capillarocopic images. The segmentation accuracy ratios of upper mentioned methods were obtainedas %80,47, %67,44, %63,23, %44,11 and 96.76%, respectively. When the results were examined, it was observed that the H-Minima method, which had not previously been applied in capillary images, reached the highest accuracy parameter value.**

Keywords: Image Processing, Capillaroscopy, Capillary Video, Capillary, Segmentation, H-Minima Method.

I. INTRODUCTION

Image segmentation is a very challenging problem that needs to be specifically designed according to the application area. The success of algorithms developed for this purpose also depends largely on the correct identification of similarity criteria used for zone homogeneity. Image segmentation techniques are often classified as threshing-based, edge determination, region-based, and clustering-based techniques [1-3].

Image segmentation, which is used in many fields, is also heavily used in the medical field and is of great importance in the diagnosis and treatment of many diseases [4]. The tests performed with a capillaroscopy device are one of these samples. Capillaroscopy is the process of taking pictures or video images of capillaries with the help of a device. With these images, capillaries are examined and changes in veins can be a precursor to some diseases. In particular, nailfold capillaroscopy makes it easy to diagnose rheumatological and diabetic diseases [5].

II. LITERATURE REVIEW

Tama et al. (2015) conducted a study to measure morphological parameters for each capillary by image processing. Morphological parameters were determined by preprocessing, dualization, skeletal (skeleton) inference and skeletal (skeleton) segmentation. These parameters are the width of the capillary, the height of the capillary, the morphology of the vascular nodes, the width of the terminal nodes, the calibre and the curvature. With the application they developed, up to 96% sensitivity was achieved in the automatic measurement of all parameters [6].

Vucic (2015) in his thesis work used the support vector machine method as an image processing technique, resulting in an accuracy parameter of 92% [7].

Bellavia et al. (2014) prefixed images with wavelet analysis and mathematical morphology. Later they applied segmentation in order to minimize in-class lighting value differences of capillary and background images. Mean sharpness, mean recall and Jaccard index were calculated as 0.924, 0.923 and 0.858, respectively [8].

Isgrò et al. (2013) also performed segmentation on sequential videos of capillaries at the tip of the nail. First, rough segmentation was applied, then a series of automatic thresholds were passed and a segmentation map was drawn with the STAPLE algorithm. The accuracy, sensitivity and authenticity parameters compared to manually segmented images were obtained as 97%, 96% and 98% respectively [9].

Goffredo et al. (2012) developed a new method for parsing the color field in digital nailfold bottom capillaroscopy analysis. The threshold values of the image were determined using Otsu technique and 7x7 median filter. In nailfold capillary images, segmentation is indicated to have the highest performance predictably in the green channel. As a result, values of 75~87%, 85~90% and >80% were found for sensitivity, authenticity and accuracy parameters, respectively [10].

Kwasnicka et al. (2007) presented a preliminary study of the use of automatic note insertion methods for computer aided diagnosis and analysis of capillary images. In summary, capillary images were taken, their features were removed, these features were processed with a predefined note splitter and they obtained an automatic note spliced capillary image. As a result of the study, five separate images were obtained. A total of six images were created with the first image passed through the Gaussian filter. These images were applied grid segmentation to create all regions together with the segmentation. After that, automatic note insertion system was applied to images using multiple class machine learning, balanced average and continuous relevance model. As a result of this application, the accuracy parameter value was obtained as 77% [11].

Riaño-Rojas et al. (2007) conducted a study to infer

segmentation and morphological features in nailfold capillaroscopic images. To segment images, the Laplace and commitment threshold of the most contrasting component in each color space have been added. Morphological feature inferences were obtained by using PCA (Principal Components Analysis), fractal geometry and tortuosity index techniques. The accuracy parameter value was calculated between 88~91%. [12].

III. MATERIAL

The intra-oral capillaroscopic images used in this study was obtained from the authors of the study of (Bellavia et al., 2014) "a non-parametric segmentation methodology for oral video-capillaroscopic images". They had ethics permission (Comitato bieoetico Dell'azienda ospedaliera Policlinico di Palermo. Verbale n.5/2012 del 16/05/2012.) for these images [13]. Necessary correspondence was provided with them and images were obtained. Additionally for this study, a GUI (Graphical User Interface) and software were implemented by using MathWorks tools of Matlab (Matrix Laboratory) package to provide segmentation of images and to make comparisons with previous studies.

IV. METHOD

In this study, previously obtained images were transferred to the developed software by MATLAB. Then the images were segmented with Otsu, Fuzzy C-mean, Fast Marching, Region Growing and H-Minima methods. The accuracy parameter ratios of the methods applied by the expert were subsequently determined by the hand segmented images (Ground Truth). The stages of this practice are as follows;

- Retrieval of the image to be processed by the software,
- Choice of method to be applied,
- Processing the image segment,
- Detection of vessel edges-boundaries by software
- Comparison of segments performed by expert and system for calculation of accuracy and other parameter values.

A. Otsu Method

This method introduces a nonparametric and unsupervised automatic threshold selection method for image segmentation. To maximize separability of the resulting classes at Gray levels, the optimal threshold is chosen by the distinguishing criterion. The procedure is very simple, using only the zero and first order cumulative moments of the gray-level histogram to perform the segmentation process. It is easy to extend the method to multivariate problems. Various experimental results have also been presented to support the validity of the method [14].

B. Fuzzy C-Mean Method

A pioneering application of fuzzy sets theory to cluster analysis was carried out by Ruspini in 1969. Until 1973, Dunn and Bezdek's work on the Fuzzy ISODATA (or fuzzy c-tool) method played an important role in the theory of cluster analysis. The important issue regarding the convergence of such methods is better understood as a result of the recent studies described in the monograph [15].

C. Fast Marching Method

FMM (Fast Marching Method) was first introduced to find numerical approximations of solutions to the stationary eiconal equation. More generally, it shows that this method allows to find solutions of numerical schemes that satisfy a definite causality conjecture. To apply this method, by presenting the shape from the shading problem, they introduced the concept of viscosity solutions in the stationary eiconal equation and took into account finite difference schemes. They also presented various comparison principles for ecological equations and schemes [16].

D. Region Growing Method

In areas such as computer image processing, image segmentation has been and is still a relevant area of research due to its widespread use and application. Image segmentation and the use of techniques in different areas have explored a review of achievements, problems encountered and open issues in the field of research. The researchers in [17] considered techniques under three groups; threshold-based, Edge-based, and Zone-based. Zone growth is an approach to image segmentation in which neighboring pixels are examined and added to a zone class if no edge is detected. This process is repeated for each border pixel in the region. If adjacent regions are found, a zone join algorithm is used where weak edges are dissolved and strong edges are left in tact. This method is very stable in terms of noise [17].

E. H-Minima Method

This method is applied before the watershed segmentation is carried out. H-minima transform is the method proposed to replace the Wolf pruning [18]. H-minima transform suppresses all regional minima in I, whose depth is less than or equivalent to H. I is the areal surface topography dataset, while H is the height threshold value (non-negative scalar) [19]. Besides, regional minima are connected components of pixels with the same dataset value, t, whose external boundary pixels all have a value greater than t [20]. To eliminate all regional minima, except the significant minima, H-minima transforms can be applied to specify a height threshold value by using the following equation:

$$H = N*Z \quad (1)$$

Where:

H = height threshold value

Z = maximum height from mean plane

N = percentage from maximum height (%)

From the Equation 1, it is observed that height threshold value depends on N (percentage of maximum height). The value of N depends on the irregularities of the measured surface topography data (~5%-20%). H-minima transform only affects the regional minima; as none of the other pixel values is changed. The significant minima remains, although their heights are increased. Moreover, the size of the significant

minima tends to increase and the number of regional minima decreases. Figure 1 shows the overview of H-minima transform function applied on the structured surface.

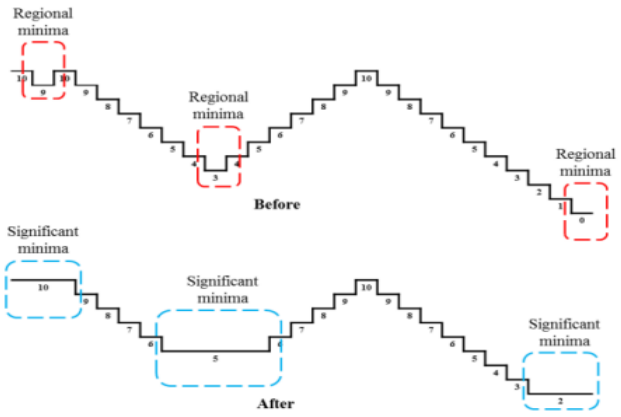

Figure 1. Overview of H-minima transform algorithm for 1-dimensional diagram. [21].

Before application of H-minima transform, numbers 9, 3, and 0 (inside the dotted red box) were the regional minima. For number 9, its depth was 1 (from 9 to 10), while for number 3, its depth was 7 (from 3 to 10), and for 0, its depth was 10 (from 1 to 10). For example, by taking 20% of the maximum height, the height threshold value becomes 2 (also called as depth). After the application of the H-minima, the result showed that H-minima transform removed all the regional minima, which were insignificant with depth smaller or equal to 2, and increased the height of the regional minima by 2. As per figure display, before and after application of H-minima transform, the regional minima (9, 3, and 0) are merged with the adjacent minima to become significant minima. Hence, all regional minima that had been less significant were transformed by 'flattening out' any insignificant regional minima into the required significant minima. Thus, H-minima transform is defined as the reconstruction by erosion of f, and increased by a height, H as in the Equation 2 [22-23]:

$$Hmin_H(f) = R_f(f + H) \quad (2)$$

Where:

$Hmin_H(f)$ = H-minima transform

$R_f(f+H)$ = reconstruction by erosion of f increases by height threshold H

F. Segmentation Flowchart

The flow diagram of the segmentation algorithm performed in this study is presented in Figure 2. Looking at the flow diagram, it is seen that the algorithm consists of three stages. The first stage is the processing of the image. At this stage, the capillaroscopic image is first uploaded to the program. The contrast values of the image are improved at the desired level and the external background images of the image to be processed are removed. The second phase involves filtering and converting. Firstly, the average filtration of the filtered image is implemented at this stage, and it is converted to the image to be processed by Otsu, Fuzzy C-mean, Fast Marching, Region Growing and H-Minima methods. In the third and final stage, the thresholds of the vessels in the image are subtracted and the vessels are determined.

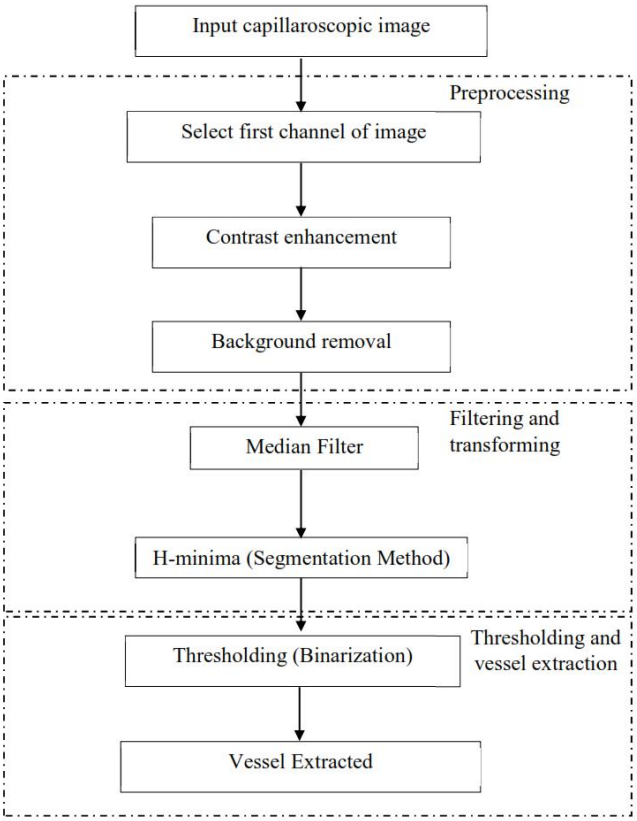

Figure 2: Segmentation flow diagram

V. Research Results and Analysis

The accuracy parameter ratios were compared with the segmented image obtained by the expert by applying Otsu, Fuzzy C-mean, Fast Marching, Region Growing and H-Minima methods. It should be noted here that H-Minima method has not been used in the studies of capillaroscopic image segmentation. After applying the segmentation methods, determination of the method with the highest accuracy parameter ratio was performed. In addition, the original images, each hand-segmented by the expert, were divided into 16 equal parts. Then, 5 methods were applied on the pictures in 1/16 scale. The accuracy parameter ratios were averaged and compared with the results obtained by application of same methods on full scale images.

The average of the results obtained by segmenting the images in the data set for Otsu, Fuzzy C-mean, Fast Marching, Region Growing and H-Minima methods are presented in Table-1.

Table 1: Segmentation parameters on full scale images

Method	Sensitivity (%)	Specificity (%)	Accuracy (%)	Processing time (Second)
Otsu	52,8952	83,1945	80,4734	0,2063
Fuzzy C-mean	6,12879	73,39620	67,44145	9,691
Fast Marching	37,39774	65,42173	63,22977	0,112
Region Growing	81,19214	39,69065	44,11263	7,294
H-Minima	81,11151	98,43124	96,75916	0,221

Table 2 includes the values of parameters of Otsu, Fuzzy C-mean, Fast Marching, Region Growing and H-Minima segmentation methods on 1/16 scale images. The values are obtained as follows:

1) Segmentation method was applied to 1/16 scale image (dividing each image into 16 equal parts on the data set)
2) The average parameters' values of segmentation is calculated for related full scale image
3) For each full scale image step 1 and step 2 were repeated
4) Final values of segmentation parameters were calculated by taking the average of parameters obtained by step 3
5) For each of 5 segmentation method step 1 to 4 were repeated

Table 2: Segmentation parameters on 1/16 scale images

Method	Sensitivity (%)	Specificity (%)	Accuracy (%)	Processing time (Second)
Otsu	47,3226	85,7178	82,1045	0,0331
Fuzzy C Mean	31,8480	75,3284	71,4306	0,3841
Fast Marching	52,8748	62,9617	62,5182	0,0105
Region Growning	74,3036	59,8206	61,7682	0,1091
H-Minima	71,1363	97,3344	94,8380	0,0713

The worst result obtained among 1/16 scale images using the H-Minima method is shown in Figure 3.

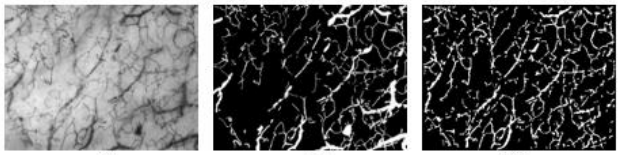

Figure 3: The worst result of the H-Minima method on 1/16 scale images; a) Original image, b) Expert hand segmentation, c) The result of the applied method

The best result obtained among 1/16 scale pictures using H-Minima method is shown in Figure 4.

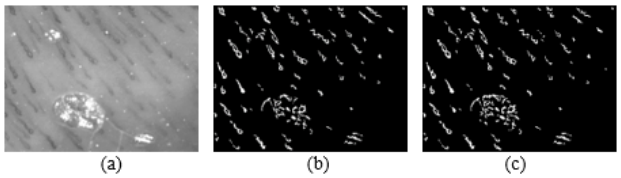

Figure 4: The best result of the H-Minima method on 1/16 scale images; a) Original image, b) Expert hand segmentation, c) The result of the applied method

A graphical comparison of the sensitivity, specificity and accuracy parameter values of the 5 segmentation methods applied on full scale images is shown in Figure 5. As can be seen from Figure 5, the highest accuracy ratio is obtained by H-Minima segmentation method.

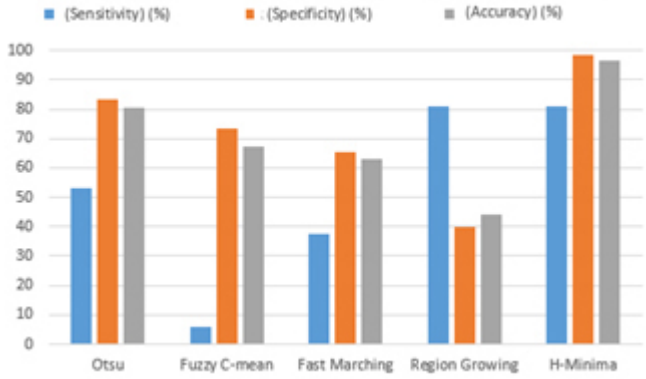

Figure 5: Comparison of all methods respect to processing time

The processing time of 5 segmentation methods is shown in Figure 6. The Fuzzy C-mean method has the maximum whereas the Otsu method has minimum processing time.

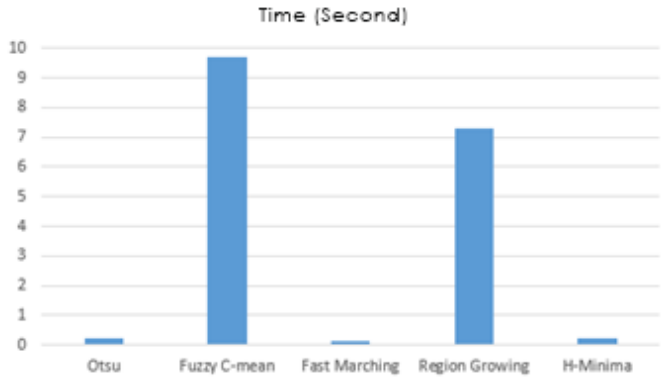

Figure 6: Processing time expenditure for all methods

VI. Results

In this study, it's aimed to develop a software for segmentation of capillaroscopic images. It includes H-minima segmentation algorithm, which had not been used before in this field. This software can contribute to the infrastructure of the decision support system to be developed for the experts of diabetic and rheumatology in the early diagnosis process and also during the treatment process.

In the software that is developed in MATLAB platform, Otsu, Fuzzy C-mean, Fast Marching, Region Growing and H-Minima methods were applied separately and the following results were obtained;

- When Otsu method was applied, the diagnostic accuracy parameter was found to be 88.6725% as maximum, 73.020% as minimum, and the average value was 80.4734%.
- When the Fuzzy C-mean method was applied, the diagnostic accuracy parameter was found to be 74.5787% as maximum and 56.7998% as minimum and the average value was 67.4414%.
- When Fast Marching method was applied, the diagnostic accuracy parameter was found to be 88,135% as maximum

and 13,5143% as minimum, and the average value was 63,2297%.

- When the Region Growing method was applied, the diagnostic accuracy parameter was found to be 86,0065% as maximum and 7,6783% as minimum and the average value was 44,1126%.
- When the H-Minima method was applied, the diagnostic accuracy parameter was found to be 99,6796% as maximum and 90,9075% as minimum and the average value was 96,7591%.

The segmentation results that are performed on 1/16 scale images are as follows;

When Otsu method was applied, the diagnostic accuracy parameter was found to be 90,2347% as maximum and 67,9906% as minimum and the average value was 82,1045%.

When the Fuzzy C-mean method was applied, the diagnostic accuracy parameter was found to be 80.7386% as maximum and 66.9137% as minimum and the average value was 71.4306%.

When Fast Marching method was applied, the diagnostic accuracy parameter was found to be 86.2718% as maximum and 49.3792% as minimum and the average value was 62.5182%.

When the Region Growing method was applied, the diagnostic accuracy parameter was found to be 88,1556% as maximum and 39,6263% as minimum, and the average value was 61,7682%.

When the H-Minima method was applied, the diagnostic accuracy parameter was found to be 97.0065% as maximum and 90.77552% as minimum and the average value was 91.7412%.

When the results in Table 3 were examined, it has been seen that the accuracy parameter ratios increased for 3 of segmentation methods namely Otsu, Fuzzy C-mean and Region Growing when 1/16 scale images were used. Fast Marching and H-Minima segmentation methods have lower accuracy ratios when it comes to 1/16 scale images. This means that the there is no generalization of increase in accuracy ratio of all segmentation methods when they are applied and combined to smaller parts of an image instead of applying full scale image itself.

Table 3: Accuracy parameter ratios of segmentation on full scale and 1/16 scale images

Method	Full scale Images	1/16 scale images	Difference (%)
	Accuracy (%)	Accuracy (%)	
Otsu	80,4734	82,1045	1,6311
Fuzzy C-mean	67,4414	71,4306	3,9892
Fast Marching	63,2297	62,5182	-0,7115
Region Growing	44,1126	61,7682	17,6556
H-Minima	96,7591	91,7412	-5,0179

In Table 4, sensitivity, specificity, accuracy and Jaccard-Index parameter values are presented in order to compare the different methods used in the literature and the H-Minima method that has not been used in the literature but in this study. It was found that H-Minima method produced compatible results with Staple (Isgrò et al. (2013)) and Wavelet Analysis (Bellavia et al. (2014)) methods.

Table 4: Comparison of H-Minima and literature studies

Researcher (Year Of Study)	Method	Sensitivity (%)	Specificity (%)	Accuracy (%)	Jaccard index
(Vucic, 2015)	Support Vector Machine	-	-	92	-
Isgrò et al. (2013)	Staple	96	98	97	-
Goffredo et al. (2012)	Otsu	75~87	85~90	>80	-
Tama et al. (2015)	Binarization	-	-	96	-
Bellavia et al. (2014)	Wavelet Analysis	92,3	92,4	-	0,858
Kwasnicka et al. (2007)	Tophat-Hessian	-	-	77	-
Riaño-Rojas et al. (2007)	Regions Growth by Threshold	-	-	88~91	-
Buber, (2019)	H-Minima	81,11	98,43	96,76	

REFERENCES

[1] Lucchese, L. ve Mitra, S. K., 2001, Colour image segmentation: a state-of-the-art survey, Proceedings-Indian National Science Academy Part A, 67 (2), 207-222.

[2] Gonzales, R., Woods, R. ve Eddins, S., 2002, Digital Image Processing, Prentice Hall, New Jersey, 567-642.

[3] Narkhede, H., 2013, Review of image segmentation techniques, International Journal of Science and Modern Engineering, 1 (8), 54-61.

[4] Altuntas, V., Altuntas, S. ve Gok, M., 2018, Automatic Colony Segmentation on Agar Surface by Image Processing.

[5] Doğdu, D. M., 2015, Bağ Dokusu Hastalıklarında Tırnak Kıvrımı Kapiller Yapısının Dermatoskop ile Değerlendirilmesi, Tıpta Uzmanlık, Selçuk Üniversitesi, Konya.

[6] Tama, A., Mengko, T. R. ve Zakaria, H., 2015, Nailfold capillaroscopy image processing for morphological parameters measurement, 2015 4th International Conference on Instrumentation, Communications, Information Technology, and Biomedical Engineering (ICICI-BME), 175-179.

[7] Vucic, V., 2015, Image Analysis for Nail-fold Capillaroscopy.

[8] Bellavia, F., Cacioppo, A., Lupaşcu, C. A., Messina, P., Scardina, G., Tegolo, D. ve Valenti, C., 2014, A non-parametric segmentation methodology for oral videocapillaroscopic images, Computer methods and programs in biomedicine, 114 (3), 240-246.

[9] Isgrò, F., Pane, F., Porzio, G., Pennarola, R. ve Pennarola, E., 2013, Segmentation of nailfold capillaries from microscopy video sequences, Proceedings of the 26th IEEE International Symposium on Computer-Based Medical Systems, 227-232.

[10] Goffredo, M., Schmid, M., Conforto, S., Amorosi, B., D'Alessio, T. ve Palma, C., 2012, Quantitative color analysis for capillaroscopy image segmentation, Medical & biological engineering & computing, 50 (6), 567-574.

[11] Kwasnicka, H., Paradowski, M. ve Borysewicz, K., 2007, Capillaroscopy image analysis as an automatic image annotation problem, 6th International Conference on Computer Information Systems and Industrial Management Applications (CISIM'07), 266-271.

[12] Riaño-Rojas, J., Prieto-Ortiz, F., Morantes, L., Sánchez-Camperos, E. ve Jaramillo-Ayerbe, F., 2007, Segmentation and extraction of morphologic

features from capillary images, 2007 Sixth Mexican International Conference on Artificial Intelligence, Special Session (MICAI), 148-159.
[13] Spera, E., Tegolo, D., & Valenti, C. (2015, June). Segmentation and feature extraction in capillaroscopic videos. In Proceedings of the 16th International Conference on Computer Systems and Technologies (pp. 244-251). ACM.
[14] Otsu, N., 1979, A threshold selection method from gray-level histograms, IEEE transactions on systems, man, and cybernetics, 9 (1), 62-66.
[15] Bezdek, J. C., 2013, Pattern recognition with fuzzy objective function algorithms, Springer Science & Business Media, p.
[16] Monneau, R., 2010, Introduction to the fast marching method.
[17] Kamdi, S. ve Krishna, R., 2012, Image segmentation and region growing algorithm, International Journal of Computer Technology and Electronics Engineering (IJCTEE), 2 (1).
[18] Wolf, G. W., 1991, A Fortran subroutine for cartographic generalization, Computers & Geosciences, 17 (10), 1359-1381.
[19] Raimondo, F., Gavrielides, M. A., Karayannopoulou, G., Lyroudia, K., Pitas, I. ve Kostopoulos, I., 2005, Automated evaluation of Her-2/neu status in breast tissue from fluorescent in situ hybridization images, IEEE Transactions on Image Processing, 14 (9), 1288-1299.
[20] C. P.Documentation and N.Agreement, "Installation Guide R 2014 b," (2014).
[21] Zaini, T. R. M., Jaafar, M., & Pin, N. C. (2016). H-minima transform for segmentation of structured surface. In MATEC Web of Conferences (Vol. 74, p. 00025). EDP Sciences.
[22] Bleau, A. ve Leon, L. J., 2000, Watershed-based segmentation and region merging, Computer Vision and Image Understanding, 77 (3), 317-370.
[23] surface topography maps," Surf. Topogr. Metrol. Prop., vol. 1, no. 1, p. 015005, Oct. (2013).